Report

Optic Flow Induces Nonvisual Self-Motion Aftereffects

Luigi F. Cuturi[1,2] and Paul R. MacNeilage[1,*]
[1]German Center for Vertigo, University Hospital of Munich, 81377 Munich, Germany
[2]Graduate School of Systemic Neurosciences, Ludwig-Maximilians University, 82152 Planegg-Martinsried, Germany

Summary

There is strong evidence of shared neurophysiological substrates for visual and vestibular processing that likely support our capacity for estimating our own movement through the environment [1, 2]. We examined behavioral consequences of these shared substrates in the form of crossmodal aftereffects. In particular, we examined whether sustained exposure to a visual self-motion stimulus (i.e., optic flow) induces a subsequent bias in nonvisual (i.e., vestibular) self-motion perception in the opposite direction in darkness. Although several previous studies have investigated self-motion aftereffects [3–6], none have demonstrated crossmodal transfer, which is the strongest proof that the adapted mechanisms are generalized for self-motion processing. The crossmodal aftereffect was quantified using a motion-nulling procedure in which observers were physically translated on a motion platform to find the movement required to cancel the visually induced aftereffect. Crossmodal transfer was elicited only with the longest-duration visual adaptor (15 s), suggesting that transfer requires sustained vection (i.e., visually induced self-motion perception). Visual-only aftereffects were also measured, but the magnitudes of visual-only and crossmodal aftereffects were not correlated, indicating distinct underlying mechanisms. We propose that crossmodal aftereffects can be understood as an example of contingent [7] or contextual adaptation [8, 9] that arises in response to correlations across signals and functions to reduce these correlations in order to increase coding efficiency. According to this view, crossmodal aftereffects in general (e.g., visual-auditory [10] or visual-tactile [11]) can be explained as accidental manifestations of mechanisms that constantly function to calibrate sensory modalities with each other as well as with the environment.

Results

Subjects seated on a hexapod motion platform in a darkened room viewed rapidly expanding or contracting optic flow patterns that simulated forward or backward linear translation at 3 m/s through a 3D cloud of randomly placed triangles (Figure 1). After 15 s of exposure, the visual stimulus was extinguished, and a physical test movement was immediately presented via the hexapod motion platform. The 2 s linear movement was in either the forward or the backward direction, and subjects indicated the perceived direction by pressing one of two buttons. This procedure was repeated 50 times per subject in three separate conditions: (1) forward

*Correspondence: paul.macneilage@lrz.uni-muenchen.de

adaptation, in which subjects adapted to expanding optic flow, (2) backward adaptation, in which they adapted to contracting optic flow, and (3) a baseline condition without visual stimuli. The magnitude of the test movement was varied after each trial according to an adaptive procedure [12] to find the physical movement that yielded a percept of zero self-motion: the point of subjective equality (PSE). This is the movement for which subjects are equally likely to respond that the movement was forward versus backward. The PSE for each subject and condition was obtained by fitting cumulative Gaussian psychometric functions using a maximum-likelihood method [13], with the PSE corresponding to the 50% point or mean parameter of the resulting fit (Figure S1 available online). All subjects provided informed written consent, and all procedures were approved by the Ethics Committee of the University Hospital of Munich.

Visual adaptation influenced subsequent nonvisual self-motion perception, as indicated by a significant difference in PSEs across conditions (repeated measures ANOVA: F = 19.86, degrees of freedom [df] = 2, p < 0.001). As a measure of the overall magnitude of the aftereffect, we took the difference between the PSEs measured in response to forward (+) and backward (−) adaptation (Figure 2A). This measure is significantly different from zero (p < 0.001), and it is positive, meaning that physical movement in the same direction as the visually simulated self-motion was required to cancel the oppositely directed aftereffects.

To separately quantify the aftereffects in the forward and backward adaptation conditions, we calculated the difference between each of these PSEs and the baseline PSE (Figure 2B). Following forward adaptation, the expected shift in the positive direction relative to baseline was observed for the majority of subjects (Figure 2B, hatched bars; mean = 1.952 cm/s). Likewise, the expected shift in the negative direction relative to baseline was also observed for the majority of subjects, following backward adaptation (Figure 2B, white bars; mean = −1.956 cm/s). These separate aftereffects in response to forward and backward visual adaptation were both significant (paired t tests; forward, p = 0.001; backward, p = 0.004). In contrast, in the baseline condition, when no adaptation stimulus preceded the physical movement, the average PSE was not significantly different from zero (Figure 2C), as expected. Baseline results were not significantly different in a control condition in which a static visual stimulus preceded the physical movement (see Supplemental Information).

As an intuitive across-subject measure of the aftereffect, we also report the percentage of times that all subjects responded forward versus backward in response to the zero-motion test stimulus. This test stimulus was naturally chosen by the adaptive procedure during all three conditions (39, 37, and 57 times during forward, backward, and baseline conditions, respectively). After forward adaptation, zero motion was perceived to be backward 66% of the time, whereas after backward adaptation, zero motion was perceived to be forward 70% of the time. These percentages are significantly higher than the expected chance outcome of 50% (binomial test: forward adaptation, p = 0.03; backward adaptation, p = 0.004). In contrast, in the baseline condition, responses did not deviate significantly from chance (57% forward responses; binomial
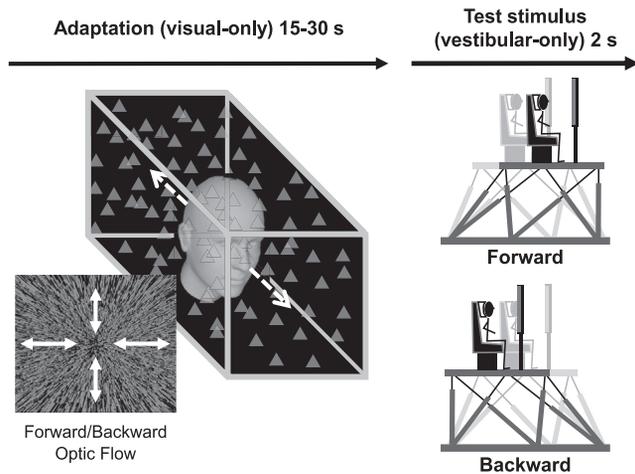
Figure 1. Experimental Setup and Trial Design

Subjects were seated on a hexapod motion platform. Viewing distance to the platform-mounted stereo visual display was ~43 cm, and field of view was ~107° × 75°. Adaptation trials began with a visual adaptation stimulus (left), simulating either forward or backward movement at 3 m/s through a volume of randomly positioned triangles, giving rise to expanding or contracting optic flow, respectively (inset). After 15 s of adaptation (30 s on the first trial), the visual stimulus was extinguished, and a transient (2 s) linear test movement was presented via the motion platform (right). The movement followed a Gaussian velocity profile (Figure S1). The subject's task was to report whether the physical test movement was forward or backward. The amplitude and direction of the test movement were varied from trial to trial, according to an adaptive procedure, and psychometric functions were fit to the resulting data (Figure S1). The mean or 50% point of the function, referred to as the PSE, provides a measure of the physical movement needed to null the visually induced aftereffect.

test, p = 0.3). Note that the zero-motion stimulus could not be recognized based on (lack of) platform vibrations because small lateral vibrations were added to all platform movements, making it impossible to use vibration as a cue (Figure S1).

We next investigated the dependence of the aftereffect on adaptor duration. We suspected that the crossmodal aftereffect depends on vection, which requires ~4–8 s of exposure for expanding or contracting optic flow [5, 14]. We therefore repeated the forward adaptation condition but with shorter-duration adaptors of 1.5 s, 3.75 s, and 7.5 s, each tested in separate blocks. Analysis across all adaptor durations revealed a significant effect (F = 4.31, df = 3, p = 0.009), but this result was due primarily to the 15 s duration condition (Figure 3A). None of the shorter-duration conditions were significantly different from baseline (1.5, p = 0.56; 3.75, p = 0.72; 7.5, p = 0.94). After each condition, we asked subjects to rate their subjective impressions of self-motion versus object motion on a scale of 1 to 7. Ratings increased with adaptor duration (Figure 3A; F = 11.72, df = 3, p < 0.001) as expected, based on prior reports [5, 14], and these ratings were correlated with aftereffect strength (r = 0.29, p = 0.016).

A final set of conditions was run to examine the relationship between the crossmodal aftereffect and the visual motion aftereffect. In these conditions, the 15 s adaptation stimuli were identical, but an optic flow test stimulus was used. The optic flow test was composed of randomly placed triangles like the adaptor, but the triangles were rendered with limited lifetime (0.5 s). The motion simulated a transient 2 s forward or backward translation through the cloud of triangles with Gaussian velocity profile, and the subject's task was to judge whether the resulting optic flow was expanding or contracting.
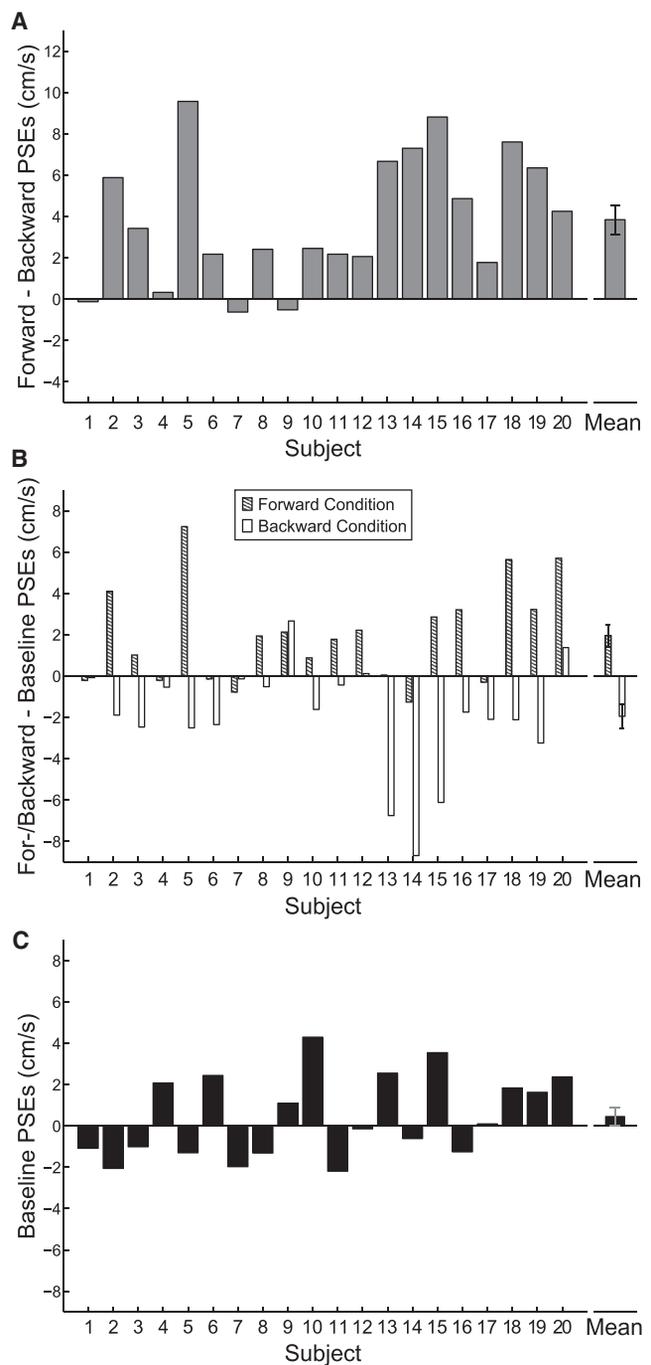
Figure 2. Crossmodal Aftereffect Results

(A) Overall magnitude of the aftereffect expressed as the difference between the PSEs measured in the forward and backward adaptation conditions. This measure is positive, meaning that a physical movement in the same direction as the adaptation stimulus was required to null the oppositely directed aftereffect.

(B) Comparison of aftereffects elicited by forward versus backward adaptation. Aftereffect size is expressed as the PSE for forward or backward adaptation minus the baseline PSE. There was no difference in the magnitude of the aftereffect elicited by forward versus backward adaptation.

(C) Baseline PSEs. In the absence of adaptation, there was no significant shift in PSEs relative to zero motion.

All error bars show SE.
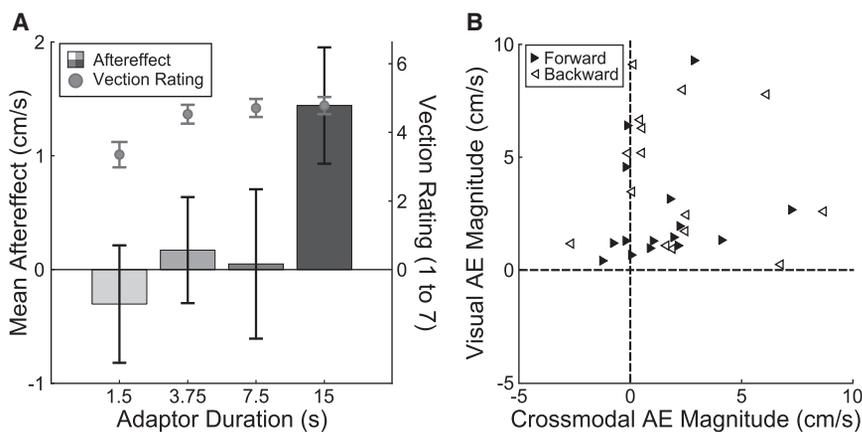
Figure 3. Effect of Adaptor Duration and Relation to Visual Aftereffect

(A) Mean crossmodal aftereffects in response to visual adaptor durations of 1.5 s, 3.75 s, 7.5 s, and 15 s. Individual subject data are shown in Figure S2. Only the 15 s condition differs significantly from zero. Gray dots indicate mean subjective ratings of vection. Ratings were given on a scale of 1 to 7, with 1 representing perception of object motion only and 7 representing perception of self-motion only. All error bars show SE.

(B) Magnitude of crossmodal versus visual-only aftereffects (forward or backward PSEs minus baseline PSEs). The two are uncorrelated. Data are normalized for adaptor direction by multiplying backward aftereffects by −1.

Significant aftereffects were observed, as expected (F = 25.0501, df = 2, p < 0.001), following both forward and backward adaptation (forward, p = 0.001; backward, p < 0.001; Figure S3B). Comparison between visual and nonvisual aftereffects after normalizing across adaptation direction revealed no significant correlation (r = 0.003, p = 0.98; Figure 3B), suggesting that these aftereffects depend on distinct underlying mechanisms. Overall, visual aftereffect magnitude was not significantly different than crossmodal (Figure 2A versus Figure S3A; p = 0.07).

Discussion

The current results show for the first time that adaptation to visual self-motion elicits an aftereffect that transfers to subsequent perception of vestibular stimulation. This crossmodal aftereffect likely results from adaptation of multisensory neural mechanisms specialized for self-motion processing. This interpretation is supported by the observation that the aftereffect was elicited only by relatively long-duration (15 s) optic flow stimulation that is known to induce sustained illusory self-motion (i.e., vection). The magnitude of the crossmodal aftereffect was not correlated with the magnitude of the purely visual motion aftereffect measured with analogous methods in the same subjects, suggesting distinct underlying mechanisms. These conclusions are developed further below in the context of prior research.

Self-Motion Aftereffects

Aftereffects have been referred to as the psychologist's microelectrode [15] because they constitute a powerful behavioral technique to investigate adaptability of neural mechanisms tuned to a given stimulus property. In particular, rigorous quantitative characterization of visual motion aftereffects has provided important clues about the neurophysiological and computational mechanisms that underlie visual motion processing [16–18]. Because visual motion is a dominant cue to self-motion, and because of compelling demonstrations of visual aftereffects particularly selective for visual self-motion stimuli (e.g., expanding and contracting optic flow [19–21]), the question has previously been raised about the possibility of analogous aftereffects for self-motion perception [3–6]. Prior studies have examined self-motion aftereffects in response to both visual [3, 5, 6] and vestibular [4, 22–24] stimuli. Many of these studies have used methods in which subjects were explicitly instructed to indicate the duration, direction, and/or magnitude of the aftereffect [3, 5, 6]. These explicit

instructions can potentially bias observer responses. In addition, magnitude estimation methods are vulnerable to individual differences in subjective scale. Under conditions of testing similar to those used here (i.e., similar adaptation duration and testing in darkness), several of these studies report persistence of motion in the adapting direction [3, 5] instead of oppositely directed aftereffects; such contradictory results may be due to methodological differences. Nulling methods like the ones employed here avoid explicit instructions regarding aftereffects and subjective scale differences and instead provide an objective metric value for aftereffect strength and direction that is suitable for interpretation in the context of computational models [11, 25, 26].

In the present study, the adapting and nulling stimuli were presented to different modalities in order to measure crossmodal transfer, which is the strongest evidence that the mechanisms under investigation are not modality specific but generalized for multisensory self-motion processing. The one prior study that employed similar methods found no consistent effects [4], most likely because an adapting stimulus with only 1.5 s duration was used. We examined the effect of adaptor duration and found significant aftereffects only with an adaptor duration of 15 s (Figure 3A). Subjective ratings of self-motion increased with adaptor duration and correlated with aftereffect magnitude. However, even though subjective ratings of self-motion were similar for the 7.5 s and 15 s conditions, and even though the 7.5 s adaptation condition should have been sufficient to elicit vection [5, 14], no aftereffect was observed. Our results therefore suggest that although vection may be necessary to induce self-motion aftereffects, as previously suggested [3, 5], it is not sufficient. Instead, sustained vection is required.

An alternative, and more trivial, explanation for the crossmodal transfer observed here would be that a visual-only aftereffect gave rise to a visual self-motion signal, which impacted perception of the nonvisual stimulus. However, this is an unlikely explanation for several reasons. First, a visual test stimulus is typically required in order to observe a visual motion aftereffect, but here, test stimuli were presented in darkness. Second, if the crossmodal aftereffect were dependent on the visual motion aftereffect, we would expect a correlation between the two, but this correlation was not observed (Figure 3B). Finally, visual motion aftereffects can be elicited with adaptor durations less than 1s [27], but the current crossmodal aftereffect was not observed for adaptor durations less than 15 s (Figure 3A). Therefore, the neural adaptation underlying the self-motion and visual motion aftereffects must be distinct.

It is safe to conclude that visual self-motion adaptation transfers to processing of self-motion stimuli from other sensory modalities. However, which modalities are most affected? Nonvisual sensation of self-motion relies on the transduction of forces applied to the head and body. The vestibular system is most specialized for transducing these stimuli for self-motion processing, but somatosensory and proprioceptive systems also respond. Crossmodal transfer between visual and somatosensory modalities has been shown previously [11]; similar interactions could potentially underlie the current results. However, discrimination of linear self-motion direction in response to small movements like the ones used here has recently been shown to depend primarily on vestibular function [28] because thresholds were significantly elevated in vestibular patients. Somatosensory thresholds can be reduced during simultaneous vestibular stimulation [29], but the most parsimonious explanation for the current results is an influence of visual adaption on perception of the vestibular stimulus.

Mechanisms of Crossmodal Adaptation

The self-motion aftereffect likely results from adaptation of neural populations sensitive to self-motion, just as visual motion aftereffects are known to result from adaptation of visual motion neurons [17]. It is widely believed that the neural adaptation underlying such aftereffects is general and widespread and functions to calibrate the system to the current range of sensory stimulation leading to improved discriminability [8, 9, 30]. Computationally, the driving force of adaptation is hypothesized to be correlations across space and time [9] or across neural units [7]. For example, a subpopulation of reciprocally connected neurons that respond maximally to a given direction of self-motion will have correlated activity during sustained self-motion in that direction. Adaptation, perhaps via mutual inhibition [7], serves to decorrelate the activity of these units. When activities are decorrelated, the neurons do not carry redundant information. Each neuron carries unique information that can aid performance (e.g., discrimination), which corresponds to an increase in coding efficiency. This structure will give rise to aftereffects when the correlations among activities of interconnected neurons changes, for example, when sustained self-motion in the subpopulation's preferred direction stops. In this case, persistence of mutual inhibition developed in response to the initial correlation leads to a bias in the perceptual readout across the whole population of self-motion sensitive neurons, i.e., an illusory percept.

Correlation-driven adaptation has most often been invoked to describe adaptation of responses to a single stimulus feature in a single modality, for example, adaptation of visual motion or orientation sensitivity [9]. However, this type of adaptation also provides a plausible explanation for crossmodal aftereffects [31]. It constitutes an automatic method to detect and adapt to naturally occurring multisensory correlations, essentially generating an efficient code for a single behaviorally relevant state variable (e.g., self-motion) out of two or more sensory signals (e.g., visual and vestibular).

Consider, for example, two populations of unimodal neurons responsive to either visual or vestibular self-motion stimuli. If these populations are reciprocally interconnected, then individual visual and vestibular neurons responsive to the same directions of visual-vestibular self-motion stimulation will have correlated activity during normal self-motion, and adaptation will function to decrease these correlations. Barlow [7] referred to this adaptation across multiple stimulus properties as contingent adaptation because it depends on the joint probability distribution across relevant properties. As in the unimodal case, adaptation serves to reduce correlations, thereby reducing redundancy and increasing coding efficiency.

In this way, correlation-driven adaptation can naturally explain the alignment of preferred visual and vestibular self-motion directions observed, for example, in area MSTd [32], a region that could potentially underlie crossmodal aftereffects. It is still unknown how the alignment of visual-vestibular tuning emerges and how activities of these populations change during adaptation. Inhibitory interactions between visual and vestibular stimulation observed in both fMRI [1] and transcranial magnetic stimulation [33] studies in humans demonstrate anatomical interconnections and mutual inhibition that could underlie correlation-driven adaptation. In general, the neural correlates of self-motion adaptation described here are a fascinating topic for future research.

In summary, crossmodal aftereffects, including those reported previously for visual-auditory [10, 34] and visual-tactile [11] interactions, are likely a byproduct of neural mechanisms constantly at work to maintain calibration across modalities. Prior demonstrations of visual-vestibular adaptation [31, 35–37] could conceivably depend on the same or similar mechanisms as those responsible for the current aftereffects. It is interesting to consider how the concept of correlation-driven neural adaptation fits with modern probabilistic approaches to modeling multimodal calibration because these models also include mechanisms by which adaptation depends on degree of crossmodal correlation [38].

References

1. Brandt, T., Bartenstein, P., Janek, A., and Dieterich, M. (1998). Reciprocal inhibitory visual-vestibular interaction. Visual motion stimulation deactivates the parieto-insular vestibular cortex. Brain *121*, 1749–1758.

2. Fetsch, C.R., Pouget, A., DeAngelis, G.C., and Angelaki, D.E. (2012). Neural correlates of reliability-based cue weighting during multisensory integration. Nat. Neurosci. *15*, 146–154.

3. Brandt, T., Dichgans, J., and Büchle, W. (1974). Motion habituation: inverted self-motion perception and optokinetic after-nystagmus. Exp. Brain Res. *21*, 337–352.

4. Crane, B.T. (2013). Limited interaction between translation and visual motion aftereffects in humans. Exp. Brain Res. *224*, 165–178.

5. Seno, T., Ito, H., and Sunaga, S. (2010). Vection aftereffects from expanding/contracting stimuli. Seeing Perceiving *23*, 273–294.

6. Patterson, R., Tripp, L., Rogers, J.A., Boydstun, A.S., and Stefik, A. (2009). Modeling the simulated real-world optic flow motion aftereffect. J. Opt. Soc. Am. A Opt. Image Sci. Vis. *26*, 1202–1211.

7. Barlow, H.B. (1990). A theory about the functional role and synaptic mechanism of visual after-effects. In Vision: Coding and Efficiency, C.B. Blakemore, ed. (Cambridge: Cambridge University Press), pp. 363–375.

8. Clifford, C.W., Webster, M.A., Stanley, G.B., Stocker, A.A., Kohn, A., Sharpee, T.O., and Schwartz, O. (2007). Visual adaptation: neural, psychological and computational aspects. Vision Res. *47*, 3125–3131.

9. Schwartz, O., Hsu, A., and Dayan, P. (2007). Space and time in visual context. Nat. Rev. Neurosci. *8*, 522–535.

10. Kitagawa, N., and Ichihara, S. (2002). Hearing visual motion in depth. Nature *416*, 172–174.

11. Konkle, T., Wang, Q., Hayward, V., and Moore, C.I. (2009). Motion aftereffects transfer between touch and vision. Curr. Biol. *19*, 745–750.

12. Kontsevich, L.L., and Tyler, C.W. (1999). Bayesian adaptive estimation of psychometric slope and threshold. Vision Res. *39*, 2729–2737.

13. Prins, N., and Kingdom, F.A.A. (2009) Palamedes: Matlab routines for analyzing psychophysical data. http://www.palamedestoolbox.org.

14. Bubka, A., Bonato, F., and Palmisano, S. (2008). Expanding and contracting optic-flow patterns and vection. Perception *37*, 704–711.

15. Frisby, J.P. (1980). Seeing: Illusion, Brain and Mind (Oxford: Oxford University Press).

16. Anstis, S., Verstraten, F.A., and Mather, G. (1998). The motion aftereffect. Trends Cogn. Sci. *2*, 111–117.

17. Mather, G., Pavan, A., Campana, G., and Casco, C. (2008). The motion aftereffect reloaded. Trends Cogn. Sci. *12*, 481–487.

18. Mather, G., Verstraten, F., and Anstis, S.M. (1998). The Motion Aftereffect: A Modern Perspective (Cambridge: MIT Press).

19. Snowden, R.J., and Milne, A.B. (1997). Phantom motion after effects—evidence of detectors for the analysis of optic flow. Curr. Biol. *7*, 717–722.

20. Morrone, M.C., Burr, D.C., Di Pietro, S., and Stefanelli, M.A. (1999). Cardinal directions for visual optic flow. Curr. Biol. *9*, 763–766.

21. Pavan, A., Marotti, R.B., and Mather, G. (2013). Motion-form interactions beyond the motion integration level: evidence for interactions between orientation and optic flow signals. J. Vis. *13*, 16.

22. Coniglio, A.J., and Crane, B.T. (2014). Human yaw rotation aftereffects with brief duration rotations are inconsistent with velocity storage. J. Assoc. Res. Otolaryngol. *15*, 305–317.

23. Crane, B.T. (2012). Fore-aft translation aftereffects. Exp. Brain Res. *219*, 477–487.

24. Crane, B.T. (2012). Roll aftereffects: influence of tilt and inter-stimulus interval. Exp. Brain Res. *223*, 89–98.

25. Carpenter-Smith, T.R., Futamura, R.G., and Parker, D.E. (1995). Inertial acceleration as a measure of linear vection: an alternative to magnitude estimation. Percept. Psychophys. *57*, 35–42.

26. Pantle, A. (1998). How do measures of the motion aftereffect measure up? In The Motion Aftereffect: A Modern Perspective, G. Mather, F. Verstraten, and S. Anstis, eds. (Cambridge: MIT Press), pp. 25–39.

27. Glasser, D.M., Tsui, J.M., Pack, C.C., and Tadin, D. (2011). Perceptual and neural consequences of rapid motion adaptation. Proc. Natl. Acad. Sci. USA *108*, E1080–E1088.

28. Valko, Y., Lewis, R.F., Priesol, A.J., and Merfeld, D.M. (2012). Vestibular labyrinth contributions to human whole-body motion discrimination. J. Neurosci. *32*, 13537–13542.

29. Ferrè, E.R., Kaliuzhna, M., Herbelin, B., Haggard, P., and Blanke, O. (2014). Vestibular-somatosensory interactions: effects of passive whole-body rotation on somatosensory detection. PLoS ONE *9*, e86379.

30. Thompson, P., and Burr, D. (2009). Visual aftereffects. Curr. Biol. *19*, R11–R14.

31. Durgin, F.H., and Gigone, K. (2007). Enhanced optic flow speed discrimination while walking: contextual tuning of visual coding. Perception *36*, 1465–1475.

32. Gu, Y., Watkins, P.V., Angelaki, D.E., and DeAngelis, G.C. (2006). Visual and nonvisual contributions to three-dimensional heading selectivity in the medial superior temporal area. J. Neurosci. *26*, 73–85.

33. Seemungal, B.M., Guzman-Lopez, J., Arshad, Q., Schultz, S.R., Walsh, V., and Yousif, N. (2013). Vestibular activation differentially modulates human early visual cortex and V5/MT excitability and response entropy. Cereb. Cortex *23*, 12–19.

34. Ehrenstein, W.H., and Reinhardt-Rutland, A.H. (1996). A cross-modal aftereffect: auditory displacement following adaptation to visual motion. Percept. Mot. Skills *82*, 23–26.

35. Bruggeman, H., Zosh, W., and Warren, W.H. (2007). Optic flow drives human visuo-locomotor adaptation. Curr. Biol. *17*, 2035–2040.

36. Rieser, J.J., Pick, H.L., Jr., Ashmead, D.H., and Garing, A.E. (1995). Calibration of human locomotion and models of perceptual-motor organization. J. Exp. Psychol. Hum. Percept. Perform. *21*, 480–497.

37. Zaidel, A., Turner, A.H., and Angelaki, D.E. (2011). Multisensory calibration is independent of cue reliability. J. Neurosci. *31*, 13949–13962.

38. Ernst, M.O., and Di Luca, M. (2011). Multisensory perception: from integration to remapping. In Sensory Cue Integration, J.K.K. Trommershauser and M.S. Landy, eds. (Oxford: Oxford University Press), pp. 224–250.